

Geometrical spin dephasing in quantum dots

Pablo San-Jose¹, Gergely Zarand^{1,2}, Alexander Shnirman¹, and Gerd Schön¹

¹ Institut für Theoretische Festkörperphysik and DFG-Center for Functional Nanostructures (CFN), Universität Karlsruhe, D-76128 Karlsruhe, Germany.

² Institute of Physics, Technical University Budapest, Budapest, H-1521, Hungary.

(Dated: February 8, 2020)

We study the relaxation and dephasing of electron spins in quantum dots that is mediated by spin-orbit coupling, and show that higher order contributions provide a relaxation mechanism that dominates in the limit of low magnetic fields. This relaxation is of geometrical origin. We further observe that in the low-field limit the relaxation processes are dominated by coupling to electron-hole excitations and possibly $1/f$ noise rather than by phonons.

PACS numbers: 03.65.Vf, 03.65.Yz, 73.21.La

Recent experiments [1, 2] demonstrate that spins of single electrons confined in quantum dot structures can be manipulated in a quantum coherent way, thus opening exciting perspectives for quantum information processing [3]. Thus a thorough understanding of spin relaxation and decoherence processes is crucial. This requires identifying the sources of fluctuations and the mechanisms how they couple to the spins, as well as analyzing the non-equilibrium decay laws. So far, two major mechanisms of dephasing have been identified: One is the hyperfine coupling to randomly oriented *nuclear spins* [4]. While in a free induction decay this leads to fast dephasing, on a time scale of order ~ 10 ns, the effect of the quasi-static nuclear field can be eliminated largely by spin-echo techniques, bringing the dephasing time into the range of $\sim 1\mu\text{s}$ [2]. The second mechanism is the coupling to (piezoelectric) phonons in the presence of *spin-orbit* interaction [5, 6, 7]. Phonons create a fluctuating electric field acting on the electrons' orbital degrees of freedom, which couples via the spin-orbit interaction to the spin. If time reversal symmetry is broken, e.g. by a magnetic field B , the process leads to spin relaxation. This decoherence mechanism is important in sufficiently strong fields [5], however, as usually described in the literature (i.e. in leading order), it is ineffective in vanishing fields.

In this paper we study, on the one hand, what processes destroy the spin coherence in vanishing or low magnetic fields. We show that higher-order virtual processes, usually neglected in the literature, provide a relaxation mechanism which *persists* as $B \rightarrow 0$. These relaxation processes are of *geometrical* origin and related to the diffusion of the Berry phase. They are the analogues of the Elliott's spin relaxation in semiconductors and metals [8], with a geometrical interpretation recently given in Ref. [9]. On the other hand, it is clear that spin relaxation is induced by *any* kind of electric field fluctuations, not merely by phonons. In fact, in order to confine, control, and measure the electron one attaches electrodes and quantum point contacts to the qubit [2]. They produce *Ohmic* fluctuations with dominant spectral weight at low frequencies. For typical quantum dots, we esti-

mate this mechanism to become relevant at low temperatures and fields below roughly 1 Tesla. In addition, the quantum point contacts produce shot noise when driven out of equilibrium, which further relaxes the spin [10]. Finally, $1/f$ background charge fluctuations, present in most mesoscopic systems, also couple to the orbital motion of the electrons and dephase the spin. In the following we shall develop a formalism that allows us to treat different types of environments on an equal footing, and also to take into account higher order virtual processes. These lead to a geometrical dephasing [11], which we estimate to be dominant below roughly 15 mTesla.

We consider a single electron confined to a lateral quantum dot by the potential $V(\vec{r})$, in the presence of a magnetic field \vec{B} . To be specific, we assume the field to be oriented parallel to the plane of the dot, but our procedure can be generalized to arbitrary directions [12]. The static part of the Hamiltonian then reads

$$H_0 = \frac{\mathbf{p}^2}{2m^*} + V(\mathbf{r}) - \frac{g\mu_B}{2}\vec{B} \cdot \vec{\sigma} + H_{SO}, \quad (1)$$

$$H_{SO} = \alpha(p_y\sigma_x - p_x\sigma_y) + \beta(p_y\sigma_y - p_x\sigma_x). \quad (2)$$

The magnetic field couples to the electron only through a Zeeman term with g -factor g [13]. The last terms describe the Dresselhaus (β) and Rashba couplings (α) between the spin $\vec{\sigma}$ of the electron and its momentum [13, 14]. For a dot of size d the typical energy of the spin-orbit coupling scales as $\sim \hbar\beta/d$, while the level spacing scales as $\delta\epsilon \sim \hbar^2/(m^*d^2)$. Therefore, for dots with small level spacing, $\delta\epsilon < 1$ K, the spin-orbit coupling cannot be treated perturbatively.

Next we account for time-dependent fluctuations of the electromagnetic field, which add a term

$$\delta V(t) = X^\mu(t) \hat{O}_\mu \quad (3)$$

to the Hamiltonian. (A summation over repeated indexes, such as μ , is assumed throughout.) The terms \hat{O}_μ denote independent operators in the Hilbert space of the confined electron (e.g., x, y, x^2, \dots), while the terms $X^\mu(t)$ denote the corresponding fluctuating (in general

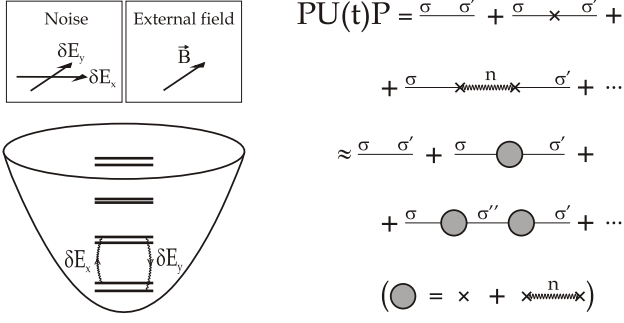


FIG. 1: Left: Single electron lateral quantum dot in a magnetic field. The ground state degeneracy is split by the magnetic field. Geometric relaxation is due to virtual transitions to excited states induced by weak fluctuations of the external fields $\delta E_x(t)$, $\delta E_y(t)$. Right: Graphical representation of the evolution operator. Virtual transitions to excited states (wavy lines) are integrated out to yield an effective Hamiltonian within the doublet subspace.

quantum) fields (e.g., δE_x , δE_y , $\nabla_x \delta E_x$, ...). They may be generated by various environments, such as phonons, localized defects, or electron-hole excitations. Information about their specific properties is contained in the spectral functions, to be specified later. Note that this formulation covers also quadrupolar fluctuations.

In case of time-reversal symmetry the ground state of the dot is two-fold degenerate. This degeneracy is split in an external magnetic field. The dynamics of the spin remains constrained to these two states as long as $g\mu_B B \ll \delta\epsilon$, $T \ll \delta\epsilon$, and the noise $\delta V(t)$ is weak. Following the method described in Ref. 15, we derive an effective Hamiltonian for the two lowest eigenstates $|\sigma = \pm\rangle$ by expanding the evolution operator $U(t) = T \exp\{-i \int_0^t dt' \delta V_{\text{int}}(t')\}$ and projecting to the subspace $\{|\sigma\rangle\}$. This yields

$$\begin{aligned} PU(t)P &= 1 - i \int_0^t dt_1 P \delta V_{\text{int}}(t_1) P \\ &\quad - \int \int_{t_1 > t_2} P \delta V_{\text{int}}(t_1) P \delta V_{\text{int}}(t_2) P \\ &\quad - \int \int_{t_1 > t_2} P \delta V_{\text{int}}(t_1) (1 - P) \delta V_{\text{int}}(t_2) P + \dots . \end{aligned} \quad (4)$$

Here $\delta V_{\text{int}}(t)$ denotes the fluctuating part of the Hamiltonian in the interaction representation and $P = \sum_\sigma |\sigma\rangle\langle\sigma|$. We separated terms that involve direct transitions between the two lowest states from transitions via excited states. In the spirit of an adiabatic approximation, these latter processes can be integrated out to yield an effective Hamiltonian in the two-dimensional subspace. Technically, this is performed by introducing slow and fast variables, $t \equiv (t_1 + t_2)/2$ and $\tau \equiv t_1 - t_2$, in the last term of Eq. (4),

$$\sim e^{-it(\epsilon_\sigma - \epsilon_{\sigma'}) - i\tau[\frac{1}{2}(\epsilon_\sigma + \epsilon_{\sigma'}) - \epsilon_n]} \delta V_{\sigma n}(t_1) \delta V_{n\sigma'}(t_2) ,$$

expanding the interaction potential in τ as $\delta V(t_{1,2}) \approx \delta V(t) \pm \frac{\tau}{2} \frac{d}{dt} \delta V(t) + \dots$, and integrating with respect to τ . Here ϵ_σ and ϵ_n denote the eigenenergies of the lowest doublet and higher eigenstates of H_0 , respectively. In this way the last term in Eq. (4) is reduced to an effective Hamiltonian that is *local in time*. As indicated in Fig. 1, this procedure can be carried out systematically to higher orders to finally yield the following effective Hamiltonian within the two-dimensional subspace represented by the pseudospin Pauli matrices $\tau_{x,y,z}$,

$$\begin{aligned} H_{\text{eff}} &= -\frac{1}{2} \vec{B}_{\text{eff}} \cdot \vec{\tau} + X^\mu \vec{C}_\mu^{(1)} \cdot \vec{\tau} + X^\mu X^\nu \vec{C}_{\mu\nu}^{(2)} \cdot \vec{\tau} \\ &\quad + \frac{1}{2} \left(\dot{X}^\mu X^\nu - X^\mu \dot{X}^\nu \right) \vec{C}_{\mu\nu}^{(3)} \cdot \vec{\tau} . \end{aligned} \quad (5)$$

The static effective field, $B_{\text{eff}} \equiv \epsilon_+ - \epsilon_-$, accounts for the usual spin-orbit renormalization of the g -factor. The couplings $\vec{C}^{(i)}$ which determine the direction and the amplitude of effective fluctuating magnetic fields felt by the pseudospin are given by

$$\left[\vec{C}_\mu^{(1)} \cdot \vec{\tau} \right]_{\sigma,\sigma'} = \hat{O}_{\sigma\sigma'}^\mu , \quad (6)$$

$$\left[\vec{C}_{\mu\nu}^{(2)} \cdot \vec{\tau} \right]_{\sigma,\sigma'} = - \sum_n' \frac{\hat{O}_{\sigma n}^\mu \hat{O}_{n\sigma'}^\nu}{\frac{\epsilon_\sigma + \epsilon_{\sigma'}}{2} - \epsilon_n} , \quad (7)$$

$$\left[\vec{C}_{\mu\nu}^{(3)} \cdot \vec{\tau} \right]_{\sigma,\sigma'} = -i \sum_n' \frac{\hat{O}_{\sigma n}^\mu \hat{O}_{n\sigma'}^\nu}{\left(\frac{\epsilon_\sigma + \epsilon_{\sigma'}}{2} - \epsilon_n \right)^2} . \quad (8)$$

The summation is restricted to excited states with $n \neq \sigma$. We do not provide explicit expressions for the eigenenergies ϵ_σ , ϵ_n , matrix elements $\hat{O}_{\sigma\sigma'}^\mu$, $\hat{O}_{\sigma n}^\mu$, or couplings $\vec{C}^{(i)}$, but below we will evaluate them numerically and provide magnitude estimates for a generic model.

In the presence of time-reversal symmetry, (i.e. $B = 0$), the first three terms of Eq. (5) vanish identically [5, 12]. Thus, only the last term survives, and it is this term that dominates the spin relaxation. It has a *geometrical* origin. To demonstrate this, let us assume that the fluctuating fields X_μ are classical, and introduce the instantaneous ground states of the Hamiltonian, $|\Phi_n(t)\rangle \equiv |\Phi_n(X_\mu(t))\rangle$ defined through the equation

$$[H_0 + \delta V(X_\mu)]|\Phi_n(X_\mu)\rangle = E_n(X_\mu)|\Phi_n(X_\mu)\rangle . \quad (9)$$

Noting that, to lowest order perturbation theory, the two degenerate instantaneous ground states are simply given by $|\Phi_\sigma(X_\mu)\rangle \approx |\sigma\rangle + \sum_n' |n\rangle\langle n| \delta V|\sigma\rangle / (\epsilon_\sigma - \epsilon_n)$, we can rewrite the last term in Eq. (5) in the familiar form

$$H_{\sigma\sigma'}^{\text{eff}}(B=0) = -i \langle \frac{d\Phi_\sigma}{dt} | \Phi_{\sigma'} \rangle , \quad (10)$$

which shows clearly that the last term is due to a Berry phase [16, 17]. In vanishing magnetic field, Eq. (10) can be shown to hold to all orders of perturbation theory [12]. The last term of Eq. (5) can cause *geometric* dephasing [11], if at least two linearly independent fluctuating

fields couple to the dot producing a random Berry phase for the spin.

The last two terms in Eq. (5) correspond to two-photon (or two phonon) processes. These have been studied before in the context of phonon-induced relaxation in electron spin resonance (ESR) experiments [18] (see also Refs. [5, 6]), however, to our knowledge, the geometric origin of the last term has not been revealed.

In the limit $B \rightarrow 0$ the Berry phase term gives the dominant relaxation mechanism. To see how geometric dephasing works, let us consider the simple case where only the electric field components δE_x and δE_y couple to the dot. Then this last term induces a random rotation of the pseudospin around $\vec{C}_{XY}^{(3)}$, by an angle proportional to the area encircled in the $(\delta E_x, \delta E_y)$ plane. As long as the fields δE_x and δE_y are linearly independent the mechanism described here leads to a spin-orbit coupling mediated geometrical spin relaxation [11, 17, 19] of the spin component perpendicular to $\vec{C}_{XY}^{(3)}$.

So far, our treatment has been rather general, and allows for the treatment of any type of noise and quantum dot. In its full glory, Eq. (5) describes the motion of the pseudo-spin coupled to three fluctuating “magnetic fields”. In general, the spin dynamics induced by these non-commuting terms in Eq. (5) is complicated. We can, however, obtain a qualitative understanding of the relevant time scales by computing the usual spin relaxation and decoherence times [20], $T_1^{(i)}$ and $T_2^{(i)}$, derived from the three terms in Eq. (5). These time scales are well-defined in the limit of sufficiently large effective fields, $B_{\text{eff}} \gg 1/T_1^{(i)}$, $1/T_2^{(i)}$. For a quantitative estimate we computed numerically the couplings $C^{(i)}$ for a parabolic confining potential, $V(\mathbf{r}) = \frac{m^* \omega_0^2}{2} |\mathbf{r}|^2$ with level spacing ω_0 and typical size $x_0 = 1/\sqrt{\omega_0 m^*}$. In this case the strength of the spin-orbit coupling is characterized by the dimensionless parameters $\tilde{\beta} \equiv \beta/x_0 \omega_0$ and $\tilde{\alpha} \equiv \alpha/x_0 \omega_0$. Furthermore, we took only dipolar fluctuations into account, choosing $\hat{O}_X \equiv x/x_0$ and $\hat{O}_Y \equiv y/x_0$ coupling to the fields $\hat{X} \equiv e\delta E_x x_0$ and $\hat{Y} \equiv e\delta E_y x_0$, respectively.

As a further approximation, we take the two components \hat{X} and \hat{Y} to be independent of each other, and assume their noise spectra to be identical, $S_X(\omega) = S_Y(\omega) = S(\omega) = \pi \varrho(\omega) \coth(\omega/2T)$, with $\varrho(\omega)$ being the spectral function of the bosonic environment (phonons or photons). The spectral function $\varrho(\omega)$ for phonons can be estimated along the lines of Ref. 5. For the parameters specified in Ref. 7 we find for piezoelectric phonons in typical GaAs heterostructures at low frequencies, $\varrho_{\text{ph}}(\omega) = x_0^2 \lambda_{\text{ph}} \omega^3$ with $\lambda_{\text{ph}} = 4 \cdot 10^{-6} \text{K}^{-2} \text{nm}^{-2}$ [12, 13]. With this parameter we obtain relaxation rates generated by the first term in Eq. (5) that coincide with those of Ref. 7 at not too high values of the field [21]. Similar values are obtained for the parameters of Ref. 22. For Ohmic fluctuations, on the other hand, the spectral function is linear at low frequencies,

$\varrho_{\Omega}(\omega) = \lambda_{\Omega} \omega$ [23, 24]. The prefactor λ_{Ω} depends on the impedance of the circuit, but for leads operated close to the pinch-off voltage we estimate it to be typically in the range $0.1 > \lambda_{\Omega} > 0.01$ [12]. For $1/f$ noise the power spectrum is $S(\omega) = \lambda_{1/f}(T)/|\omega|$. The temperature-dependent coefficient $\lambda_{1/f}(T)$ is frequently found to scale as $\lambda_{1/f}(T) \sim T^2$ at $T > 100 \text{ mK}$ [25, 26, 27], while it saturates at lower temperatures.

The three terms in Eq. (5) lead to different types of relaxation. The coupling $\vec{C}^{(1)}$ turns out to be always exactly perpendicular to \vec{B}_{eff} [7], and for low magnetic fields and weak spin-orbit coupling is proportional to $|\vec{C}^{(1)}| \sim \frac{B}{\delta\epsilon} \max\{\tilde{\alpha}, \tilde{\beta}\}$. This fluctuating field therefore contributes to the T_1 -relaxation only,

$$1/T_1^{(1)} = 2 \left(|\vec{C}_X^{(1)}|^2 + |\vec{C}_Y^{(1)}|^2 \right) S_X(B_{\text{eff}}). \quad (11)$$

It roughly scales as $1/T_1^{(1)} \sim B^2 \max\{B, T\}$ for Ohmic dissipation and as $\sim B^4 \max\{B, T\}$ for phonons. As a consequence, we find that for typical dots with level spacing in the range $\delta\epsilon \approx 1 \dots 10 \text{ K}$ Ohmic fluctuations dominate over phonons for fields in the range $B < 1 \dots 3 \text{ T}$.

The second term, $|\vec{C}^{(2)}| \sim \frac{B}{(\delta\epsilon)^2} \max\{\tilde{\alpha}^2, \tilde{\beta}^2\}$ [30] contributes to both T_1 and T_2 , and in fact, this is the term that provides the leading contribution to the “pure dephasing” rate, $1/T_2^*$ [20]. The spin relaxation rate corresponding to this term can be expressed as

$$\frac{1}{T_1^{(2)}} = 4 \left(|\vec{C}_{XX,s}^{(2,\perp)}|^2 + |\vec{C}_{YY,s}^{(2,\perp)}|^2 + 2|\vec{C}_{XY,s}^{(2,\perp)}|^2 \right) S_{XY}(B_{\text{eff}}),$$

$$S_{XY}(\omega) = \frac{\pi}{2} \int d\tilde{\omega} \frac{\varrho(\frac{\omega+\tilde{\omega}}{2}) \varrho(\frac{\omega-\tilde{\omega}}{2})}{1 - \cosh(\tilde{\omega}/2T) / \cosh(\omega/2T)}, \quad (12)$$

with $\vec{C}_{\mu\nu,s}^{(2,\perp)}$ denoting the symmetrized component of $\vec{C}_{\mu\nu}^{(2)}$ perpendicular to \vec{B}_{eff} . Correspondingly, for Ohmic dissipation $1/T_1^{(2)}$ vanishes as $\sim B^2 \max\{B^3, T^3\}$, while for phonons it is $\sim B^2 \max\{B^7, T^7\}$.

Finally, for an in-plane magnetic field, $\vec{C}^{(3)}$ is also perpendicular to \vec{B}_{eff} and remains constant as $B \rightarrow 0$. Its contribution to the geometrical relaxation is

$$1/T_1^{(3)} = 2|\vec{C}_{XY,a}^{(3)}|^2 S_{\hat{X}Y-\hat{X}\hat{Y}}(B_{\text{eff}}), \quad (13)$$

$$S_{\hat{X}Y-\hat{X}\hat{Y}}(\omega) = \frac{\pi}{2} \int d\tilde{\omega} \frac{\tilde{\omega}^2 \varrho(\frac{\omega+\tilde{\omega}}{2}) \varrho(\frac{\omega-\tilde{\omega}}{2})}{1 - \cosh(\tilde{\omega}/2T) / \cosh(\omega/2T)},$$

with $\vec{C}_{\mu\nu,a}^{(3)}$ being the anti-symmetrized component of $\vec{C}_{\mu\nu}^{(3)}$.

Most important, with $|\vec{C}_{XY}^{(3)}| \sim \frac{1}{(\delta\epsilon)^2} \max\{\tilde{\alpha}^2, \tilde{\beta}^2\}$, the rate $1/T_1^{(3)}$ approaches a constant value at finite temperatures as $B \rightarrow 0$, and scales as $\sim \max\{B^5, T^5\}$ for Ohmic dissipation and $\sim \max\{B^9, T^9\}$ for phonons.

The relaxation rates corresponding to the different terms in Eq. (5) and various noise sources are shown in

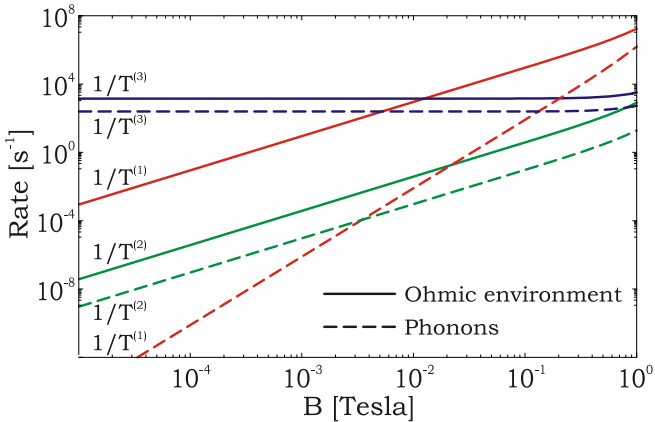


FIG. 2: Spin relaxation rates for a GaMnAs quantum dot with level spacing $\omega_0 = 1\text{K}$ as function of the Zeeman field. We chose a temperature $T = 100\text{ mK}$ and Ohmic coupling $\lambda_\Omega = 0.05$. Below $B^* \approx 1\text{ T}$ spin relaxation is dominated by coupling to Ohmic fluctuations. For $B < B^{**} \approx 15\text{ mT}$ geometrical spin relaxation due to coupling to Ohmic fluctuations dominates. For all B values plotted, the Bloch-Redfield consistency requirement, $B_{\text{eff}} \gg 1/T^{(i)}$, is satisfied.

Fig. 2. Clearly, for external fields $B < B^* \approx 1 \dots 3\text{ T}$ Ohmic fluctuations provide the leading relaxation mechanism. The value of the crossover field B^* is not very sensitive to the specific value of the spectral parameter λ_Ω and is independent of the spin-orbit coupling. Below a second crossover field, $B^{**} \approx 15\text{ mT}$, the geometric dephasing (spin relaxation) induced by Ohmic fluctuations starts to dominate. This second crossover scale is, however, very sensitive to the spin-orbit coupling and temperature, scaling as $B^{**} \sim \max\{\tilde{\alpha}, \tilde{\beta}\}\omega_0(T/\omega_0)^2$. E.g. for a level spacing $\delta\epsilon \sim \omega_0 \sim 1\text{K}$ the Berry phase mechanism gives a relaxation rate of the order of $700\text{ }\mu\text{s}$ (20 ms) at a temperature $T = 100\text{ mK}$ ($T = 50\text{ mK}$). For even lower temperatures or smaller dots with level spacing $\delta\epsilon \sim 10\text{K}$ the $B \rightarrow 0$ relaxation time is quickly pushed up to the range of several seconds.

Finally, we comment on the effect of $1/f$ noise. In most cases, the non-symmetrized correlators for $1/f$ noise, needed to calculate correlators as S_{XY} or S_{XX} , are not known. Yet, for $|\omega| \ll T$ we can provide an

estimate $S_{XY}(\omega) \approx \int_{-T}^T \frac{d\tilde{\omega}}{2\pi} S_X(\omega - \tilde{\omega}) S_Y(\tilde{\omega})$, and similarly for $S_{\dot{X}Y - X\dot{Y}}$. The $B = 0$ geometrical relaxation rate due to the $1/f$ noise can be estimated as $|\tilde{C}_{XY}^{(3)}|^2 \lambda_{1/f}^2(T) \omega_c$, where ω_c is the upper frequency cut-off for the $1/f$ noise [28]. Accounting for the high-frequency (Ohmic) noise, sometimes observed to be associated with the $1/f$ noise [25, 26, 27, 29], the estimate becomes $|\tilde{C}_{XY}^{(3)}|^2 \lambda_{1/f}^2(T) (k_B T / \hbar)$. While the $1/f$ noise of background charge fluctuations is well studied in mesoscopic systems, the amplitude of the $1/f$ noise of the electric field in quantum dot systems is yet to be determined.

If we assume that this noise is due to two-level systems at the interfaces of the top gate electrodes, we conclude that in the parameter range explored here, the effect of $1/f$ noise is less important than that of Ohmic fluctuations. However, in quantum dots with large level spacings in the low-temperature and low-field regime, these fluctuations could dominate over the effect of Ohmic fluctuations and eventually determine the spin relaxation time.

We thank J. Fabian for valuable discussions. This work is part of a research network of the Landesstiftung Baden-Württemberg gGmbH. It has been supported by Hungarian Grants OTKA Nos. NF061726, T046267, and T046303, and the SQUBIT2 project IST-2001-39083.

- [1] J. M. Elzerman *et al.*, Nature **430**, 431 (2004).
- [2] J. R. Petta *et al.*, Science **309**, 2180 (2005).
- [3] D. Loss and D. P. DiVincenzo, Phys. Rev. A **57**, 120 (1998).
- [4] A. V. Khaetskii, D. Loss, and L. Glazman, Phys. Rev. Lett. **88**, 186802 (2002).
- [5] A. V. Khaetskii and Y. V. Nazarov, Phys. Rev. B **6412**, 125316 (2001).
- [6] L. M. Woods, T. L. Reinecke, and Y. Lyanda-Geller, Phys. Rev. B **66**, 161318 (2002).
- [7] V. N. Golovach, A. Khaetskii, and D. Loss, Phys. Rev. Lett. **93**, 016601 (2004).
- [8] R. J. Elliott, Phys. Rev. **96**, 266 (1954).
- [9] Y. A. Serebrennikov, Phys. Rev. Lett. **93**, 266601 (2004).
- [10] M. Borhani, V. N. Golovach, and D. Loss, cond-mat/0510758.
- [11] R. S. Whitney, Y. Makhlin, A. Shnirman, and Y. Gefen, Phys. Rev. Lett. **94**, 070407 (2005).
- [12] P. San-Jose *et al.*, to be published.
- [13] For GaAs $m^* \approx 0.067 m_e$, $g \approx 0.44$, sound velocities for longitudinal and transverse modes $v_l = 4.73 \cdot 10^3 \text{ m/s}$ and $v_t = 3.35 \cdot 10^3 \text{ m/s}$, piezoelectric constant $h_{14} = 1.4 \cdot 10^9 \text{ eV/m}$, density $\rho = 5.3 \cdot 10^3 \text{ Kg/m}^3$, $\lambda_{ph} = [(e^2 h_{14}^2 / 105(2\pi)^2 \rho) (3/v_l^5 + 4/v_t^5)]$. For the numerical calculation we assumed only Dresselhaus coupling with $\lambda_{SO} = x_0/\tilde{\beta} = 1\mu\text{m}$.
- [14] R. Winkler, *Spin-orbit coupling effects in two-dimensional electron and hole systems*, Springer Tracts in Modern Physics (2003).
- [15] C. Hutter, A. Shnirman, Y. Makhlin, and G. Schön, cond-mat/0602086.
- [16] M. V. Berry, Proc. R. Soc. London A **392**, 45 (1984).
- [17] F. Wilczek and A. Zee, Phys. Rev. Lett. **52**, 2111 (1984).
- [18] E. Abrahams, Phys. Rev. **1**, 491 (1957).
- [19] C. A. Mead, Phys. Rev. Lett. **59**, 161 (1987).
- [20] F. Bloch, Phys. Rev. **105**, 1206 (1957).
- [21] For larger frequencies the approximation $\varrho_{ph}(\omega) = x_0^2 \lambda_\Omega \omega^3$ is not valid since the wavelength of relevant phonons becomes comparable to the size of the dot.
- [22] P. Stano and J. Fabian, cond-mat/0512713.
- [23] A. J. Leggett *et al.*, Rev. Mod. Phys. **59**, 1 (1987).
- [24] U. Weiss, *Quantum dissipative systems* (World Scientific, Singapore, 1999), 2nd ed.
- [25] O. Astafiev, Y. A. Pashkin, Y. Nakamura, T. Yamamoto, and J. S. Tsai, Phys. Rev. Lett. **93**, 267007 (2004).

- [26] A. Shnirman, G. Schön, I. Martin, and Y. Makhlin, Phys. Rev. Lett. **94**, 127002 (2005).
- [27] O. Astafiev *et al.*, Phys. Rev. Lett., in print.
- [28] G. Ithier *et al.*, Phys. Rev. B **72**, 134519 (2005).
- [29] L. Faoro, J. Bergli, B. L. Altshuler, and Y. M. Galperin, Phys. Rev. Lett. **95**, 046805 (2005).
- [30] Note that there is no discrepancy with the scaling $\max\{\tilde{\alpha}, \tilde{\beta}\}$ quoted in Ref. 5, since they include higher (multipolar) spin-flipping phonon contributions neglected here.